Kvak, R., Zacharov, P., 2026. Environmental Precursors of Convective Storms in the ALADIN Reanalysis. In: Tolasz, R., Šustková, V. (Ed.), Proceedings of the 2nd PERUN Project Conference (TA ČR, SS02030040). CHMI, Praha, pp. 37–45, ISBN 978-80-7653-095-9. https://doi.org/10.59984/978-80-7653-095-9.05

Environmental Precursors of Convective Storms in the ALADIN Reanalysis

(Prekurzory prostredia konvektívnych búrok v reanalýze ALADIN)

Kvak, R., Zacharov, P.

https://doi.org/10.59984/978-80-7653-095-9.05

Róbert Kvak, Institute of Atmospheric Physics CAS, kvak@ufa.cas.cz

Petr Zacharov, Institute of Atmospheric Physics CAS, petas@ufa.cas.cz

Abstract: Within the PERUN project, we evaluated how well an ALADIN-based reanalysis represents atmospheric conditions favourable for the development of convective storms, including severe and organized convection. The spatiotemporal analysis over Central Europe and adjacent regions focused on two key diagnostic variables widely used in operational forecasting and climatological studies: (i) convective available potential energy of the most unstable parcel in the lower troposphere (MUCAPE) and (ii) 0–6 km above-ground-level bulk wind shear. Outputs from the regional reanalysis with a horizontal grid spacing of 2.3 km were compared with the global ERA5 reanalysis at a resolution of 0.25°. The performance of both reanalyses was evaluated against radiosonde observations from the Praha–Libuš station using a long-term observational record covering 1992–2019. In addition, the spatial distribution and seasonal variability of MUCAPE and wind-shear fields over a broader Central European domain were examined using daily data for 1991–2020. The combined comparison of the regional and global reanalyses with station observations makes it possible to identify the strengths and limitations of regional reanalysis relative to global reanalysis in representing convective potential and environmental conditions supporting organized convection. The results are relevant to convective climatology, model validation, and long-term assessments of hazards associated with severe convection.

Keywords: convective environment – regional reanalysis – severe convection – complex terrain

Abstrakt: V rámci projektu PERUN sa hodnotila reprezentatívnosť atmosférických podmienok v reanalýze založenej na modeli ALADIN, ktoré sú priaznivé pre vznik konvektívnych búrok vrátane silnej a organizovanej konvekcie. Časopriestorová analýza nad strednou Európou a priľahlými regiónmi sa zamerala na dve kľúčové diagnostické premenné konvektívneho prostredia, bežne využívané v operatívnej predpovedi aj klimatologických štúdiách: (i) konvektívnu dostupnú potenciálnu energiu najnestabilnejšej vzduchovej častice v spodných vrstvách (MUCAPE) a (ii) strih vetra vo vrstve 0–6 km nad zemským povrchom. Výstupy regionálnej reanalýzy s horizontálnym rozlíšením 2,3 km sa porovnali s globálnou reanalýzou ERA5 (rozlíšenie 0,25°). Kvalita reanalýz bola overená porovnaním s aerologickými meraniami zo stanice Praha-Libuš na základe dlhodobého radu pozorovaní za obdobie 1992–2019. Súčasne sa skúmalo priestorové rozloženie a sezónna variabilita polí MUCAPE a strihu vetra nad širšou doménou strednej Európy na základe denných údajov za obdobie 1991–2020. Kombinácia porovnania výstupov regionálnej a globálnej reanalýzy so staničnými pozorovaniami umožňuje identifikovať prednosti aj limity regionálnych oproti globálnym reanalýzam pri zachytení konvektívneho potenciálu a podmienok podporujúcich organizovanú konvekciu. Výsledky sú relevantné pre klimatológiu, validáciu modelov a dlhodobé hodnotenie rizika výskytu nebezpečných javov spojených so silnou konvekciou.

Kľúčová slova: konvektívne prostredie – regionálna reanalýza – silná konvekcia – zložitý terén

Introduction

Convective storms are among the most significant warm-season weather phenomena in Europe (Taszarek et al. 2019). Although they usually affect limited areas and have short lifetimes, they can produce hail, damaging winds, intense rainfall, lightning, and occasionally tornadoes. Their rapid development, small spatial scale, and strong sensitivity to local atmospheric conditions make their prediction and climatological assessment particularly challenging (Groenemeijer et al. 2017; Fischer et al. 2025). Severe convective storms also cause casualties and substantial economic losses in Central Europe, highlighting the need for reliable information on the environments in which they develop (e.g., Púčik et al. 2019; Kühne et al. 2025).

The development and severity of convective storms depend on the simultaneous presence of sufficient moisture, instability, a lifting mechanism, and, particularly for organized convection, favorable vertical wind profiles (Doswell et al. 1996; Nelson et al. 2021). Convective available potential energy (CAPE) and vertical wind shear are therefore among the most widely used thermodynamic and kinematic diagnostics of convective environments. Most-unstable CAPE (MUCAPE) represents the buoyant energy available to the most unstable parcel within a specified lower-tropospheric layer. It can characterize both surface-based and elevated instability and provides an estimate of the potential strength of convective updrafts (Ribeiro and Bosart 2018). The 0–6 km above-ground-level bulk wind shear is associated with updraft–downdraft separation, storm longevity and organization, and supercell potential (e.g., Mulholland et al. 2018; Trapp et al. 2020). Combining instability and deep-layer shear consequently provides more information on the potential for severe and organized convection than either parameter considered separately (Sherburn and Parker 2014; Taszarek et al. 2017).

Because long-term, spatially homogeneous observations of individual convective hazards remain limited (Dotzek et al. 2009; Kvak et al. 2023), analyses of storm-supporting environments provide a useful indirect approach to assessing where and how frequently potentially hazardous convection may occur. High-resolution regional datasets are particularly valuable over Central Europe, where complex terrain produces pronounced spatial variations in temperature, moisture, wind, and convective initiation (Kvak and Kašpar 2026). Orographic lifting and terrain-induced circulations can locally modify instability and vertical wind profiles, whereas coarser datasets may smooth the terrain and associated mesoscale gradients (e.g., Taszarek et al. 2018; 2020).

The aim of this contribution is to evaluate MUCAPE derived from the 2.3 km ALADIN regional reanalysis against radiosonde observations from Praha-Libuš during 1992–2019 and to describe the spatial distribution of environments favorable for strong and organized convection over the Czech Republic, Slovakia, and surrounding regions using MUCAPE and 0–6 km bulk wind shear. Section 2 describes the data and methods, Section 3 presents and discusses the results, and Section 4 summarizes the main conclusions.

Data and methods

The present analysis was based on a regional reanalysis produced using the ALADIN-Climate model in the ALARO configuration. The reanalysis has a horizontal grid spacing of 2.3 km and 87 vertical levels extending from the surface to approximately 53 km over an extended Central European domain. It employs a non-hydrostatic, fully compressible dynamical core, while partly resolved and subgrid-scale deep convection is represented using the Modular Multiscale Microphysics and Transport (3MT) scheme. The data assimilation system operates in 6-h cycles at 00, 06, 12, and 18 UTC. Surface observations are assimilated using optimal interpolation, whereas the upper-air state is generated using Digital Filter Blending. Forecasts initialized at 00 UTC are integrated for 30 h and provide hourly output fields.

MUCAPE from the ALADIN reanalysis was evaluated against radiosonde observations from Praha-Libuš, Czech Republic (WMO station 11520), the primary upper-air station operated by the Czech Hydrometeorological Institute, for 1992–2019, during which radiosonde data were available. The soundings provide vertical profiles of pressure, temperature, humidity, and wind, generally at 00 and 12 UTC, with occasional intermediate soundings at 06 and 18 UTC. Reanalysis values from the nearest grid point were matched with observations at all corresponding valid times. MUCAPE was calculated for the most unstable parcel within the lowest 300 hPa, while the 0–6 km bulk wind shear was calculated as the vector difference between the near-surface wind and the wind at 6 km above ground level.

The spatial analysis covered the Czech Republic, Slovakia, and neighboring regions over the full 30-year period from 1991 to 2020. At each grid point, the 95th percentile of daily maximum MUCAPE was calculated. The mean annual number of days satisfying selected combinations of MUCAPE and 0–6-km bulk wind shear was also determined. A day was counted when both criteria were satisfied simultaneously in the same hourly model field. The selected thresholds were intended to distinguish broad convective-environment regimes rather than to determine storm mode explicitly. Deep-layer shear of 10–20 $m \cdot s^{-1}$ generally supports multicellular and other organized convection, whereas shear $\geq$ 20 $m \cdot s^{-1}$ is more favorable for persistent organized storms, including supercells (Doswell et al. 1996). The MUCAPE intervals represent moderate, high, and very high instability. They allow strong-shear environments to be compared across different instability levels and very-high-instability environments under moderate and strong shear. Because all combinations require at least 10 $m \cdot s^{-1}$ of shear, weak-shear environments more commonly associated with short-lived single-cell convection are largely excluded.

Results and discussion

The comparison shown in Fig. 1 comprised 22 178 matched reanalysis and sounding profiles from Praha-Libuš. ALADIN and the observations were assigned to the same MUCAPE category in 65.2% of cases, although this agreement was dominated by the most frequently occurring lowest category. The reanalysis indicated a higher category than the sounding in 26.2% of cases and a lower category in only 8.7%, suggesting an overall shift toward higher MUCAPE values. The lowest category, MUCAPE < 40 $J \cdot kg^{-1}$, accounted for 49.4% of the reanalysis profiles but 59.0% of the soundings. Conversely, MUCAPE $\geq$ 800 $J \cdot kg^{-1}$ occurred in 9.2% of the reanalysis profiles and 6.0% of the soundings. Nevertheless, 77.6% of the observed cases with MUCAPE $\geq$ 800 $J \cdot kg^{-1}$ were also assigned to the highest category by ALADIN. The reanalysis therefore identified most strongly unstable observed environments, although their frequency appears to be overestimated at Praha-Libuš.

Part of the disagreement may result from the sensitivity of MUCAPE to relatively small differences in lower-tropospheric temperature and moisture and from comparing a point sounding with a model grid box. Previous comparisons have generally found larger reanalysis differences for thermodynamic parcel parameters than for kinematic parameters, with additional representativeness issues possible near complex terrain (e.g., Taszarek et al. 2018). Conversely, a fixed-site sounding samples only one atmospheric profile and may not represent nearby mesoscale variability or the environment closest to developing convection (e.g., Nelson et al. 2021).

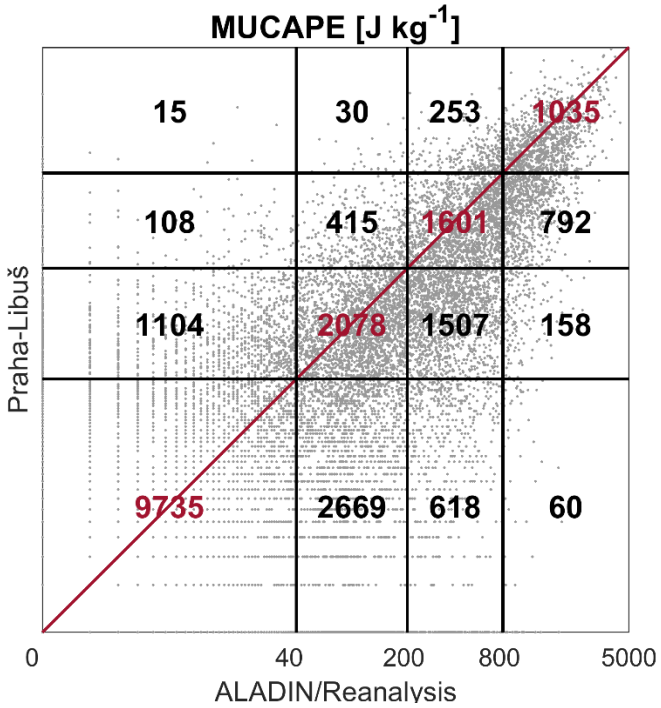


Fig. 1. Joint frequency distribution of MUCAPE from Praha–Libuš soundings and collocated ALADIN reanalysis profiles during 1992–2019. Numbers indicate sample counts within categories bounded by 40, 200, and 800 J·kg⁻¹. The red line and numbers denote 1:1 agreement in given category.

The spatial distribution of the 95th percentile of daily maximum MUCAPE shows substantial variability (Fig. 2). Values generally range from approximately 1500 to 2300 J·kg⁻¹ across the Czech Republic. Lower values occur over elevated areas in western and northern Czechia, whereas higher values extend across southern Moravia and parts of southern Czechia. In Slovakia, values below approximately 1800 J·kg⁻¹ follow the higher Carpathian terrain, while the southern and eastern basins and lowlands locally exceed 2500 J·kg⁻¹. Comparable or higher values occur in the neighboring Pannonian Basin, the northeastern Alpine foreland, and parts of southern Poland. The pronounced gradients between mountain ridges, basins, and lowlands demonstrate the fine spatial structure represented by the 2.3 km reanalysis, which may be smoothed in coarser global reanalyses (e.g., Taszarek et al. 2020).

High MUCAPE should not, however, be interpreted as a direct measure of the frequency of convective storms. Lowlands may support greater buoyancy because of warmer and moister lower-tropospheric conditions, while mountainous regions may experience more frequent convective initiation through orographic lifting and terrain-induced convergence (Mulholland et al. 2018; Kvak and Kašpar 2026). This distinction may explain why observed thunderstorm climatologies identify the Alps, Carpathians, and their foothills as regions of frequent storm activity, whereas the highest MUCAPE values in Fig. 2 are often located in adjacent lowlands (e.g., Taszarek et al. 2019). The comparison at Praha-Libuš (Fig. 1) also suggests that the mapped frequency of high-MUCAPE environments may be somewhat overestimated, although observations from a single station cannot establish a domain-wide bias.

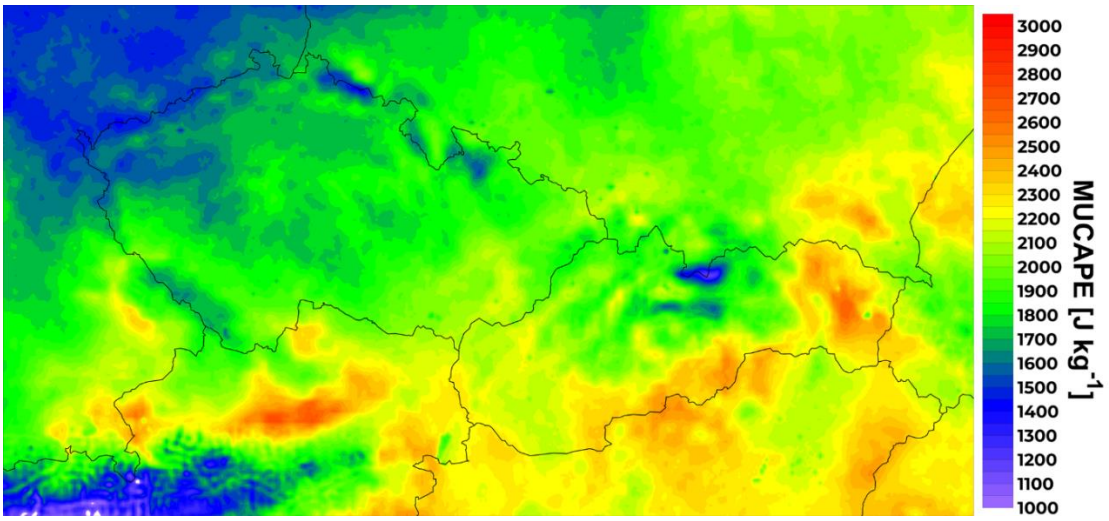


Fig. 2. Spatial distribution of the 95th percentile of daily maximum MUCAPE during 1991–2020 over the Czech Republic, Slovakia, and adjacent regions.

Figures 3–6 show that environments supportive of organized and severe convection become progressively less frequent as the combined instability and shear thresholds increase. Under strong 0–6 km bulk wind shear of at least 20 m·s^{-1}, environments with 500 ≤ MUCAPE < 1000 J·kg^{-1} are the most frequent, generally occurring on approximately 2–4 days·yr^{-1} and locally reaching about 5 days·yr^{-1}, particularly near elevated terrain and over parts of the German lowlands (Fig. 3). Their frequency decreases mostly to 1–3 days·yr^{-1} when MUCAPE increases to 1000–2000 J·kg^{-1} (Fig. 4). Environments with MUCAPE ≥ 2000 J·kg^{-1} occur more frequently with moderate shear of 10–20 m·s^{-1} than with shear ≥ 20 m·s^{-1}. The moderate-shear combination generally occurs on approximately 0.5–2 days·yr^{-1}, with localized frequencies of 3 days·yr^{-1} or more in parts of the Alpine foreland and eastern Slovakia (Fig. 5). By contrast, the simultaneous occurrence of MUCAPE ≥ 2000 J·kg^{-1} and shear ≥ 20 m·s^{-1} remains below 1 day·yr^{-1} across most of the Czech Republic and Slovakia (Fig. 6). Frequencies locally reach approximately 1–1.5 days·yr^{-1} near the Bohemian Forest, about 2 days·yr^{-1} in parts of eastern Slovakia, and approximately 2.5 days·yr^{-1} in the eastern Alpine foreland near the Austria–Hungary border.

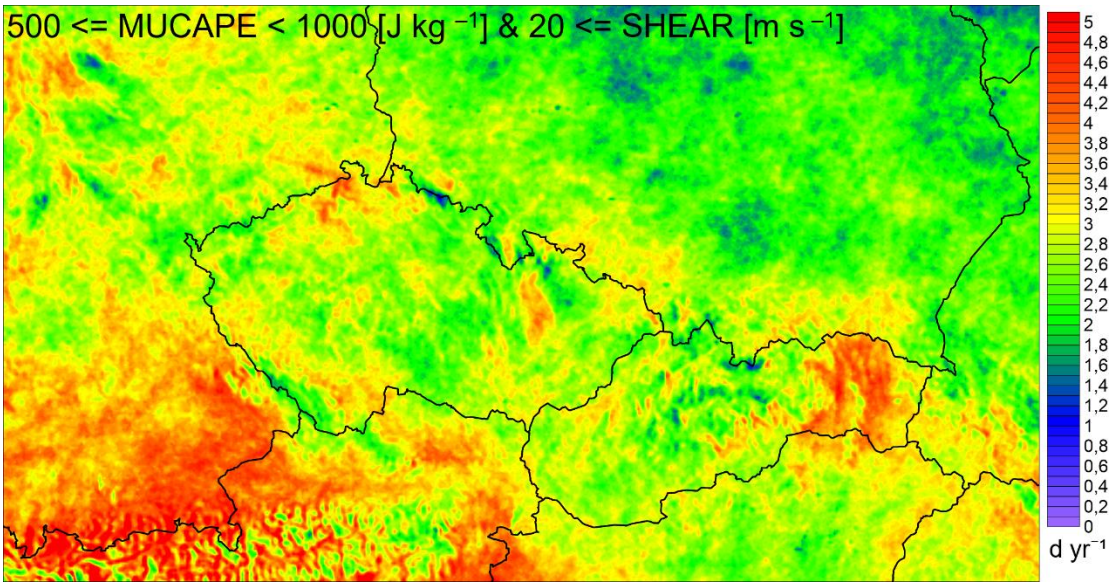


Fig. 3. Mean annual number of days during 1991–2020 on which MUCAPE and 0–6-km bulk wind shear (SHEAR) simultaneously satisfied the criteria specified in the figure title.

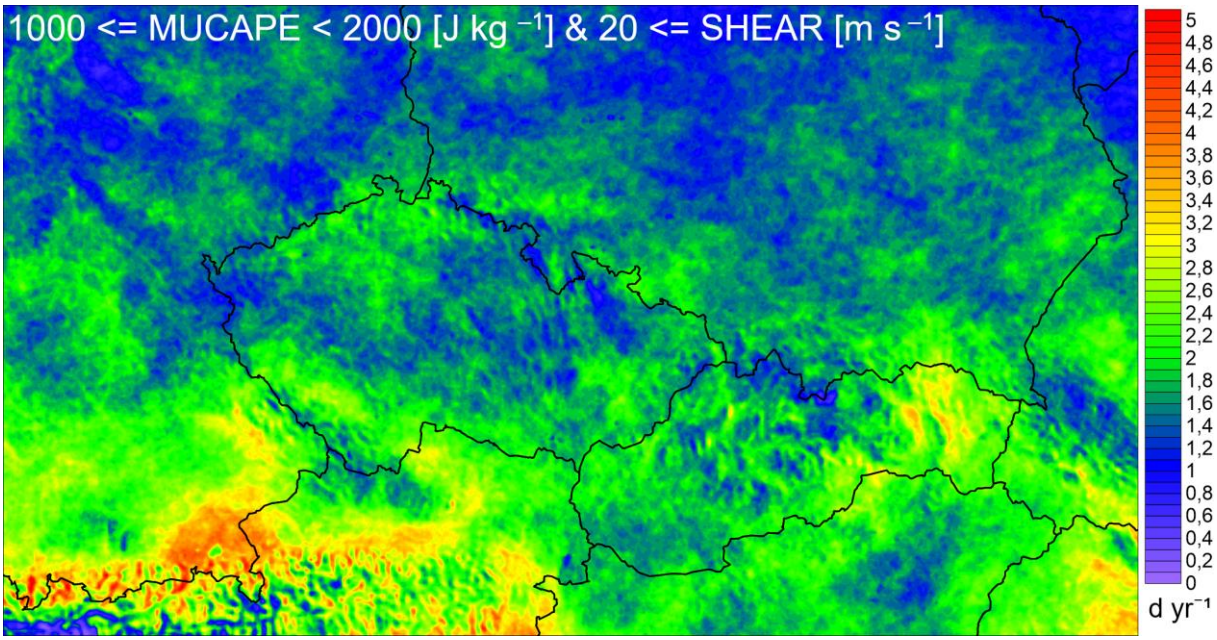


Fig. 4. As in Fig. 3, but for the MUCAPE and 0–6-km bulk wind shear criteria specified in the figure title.

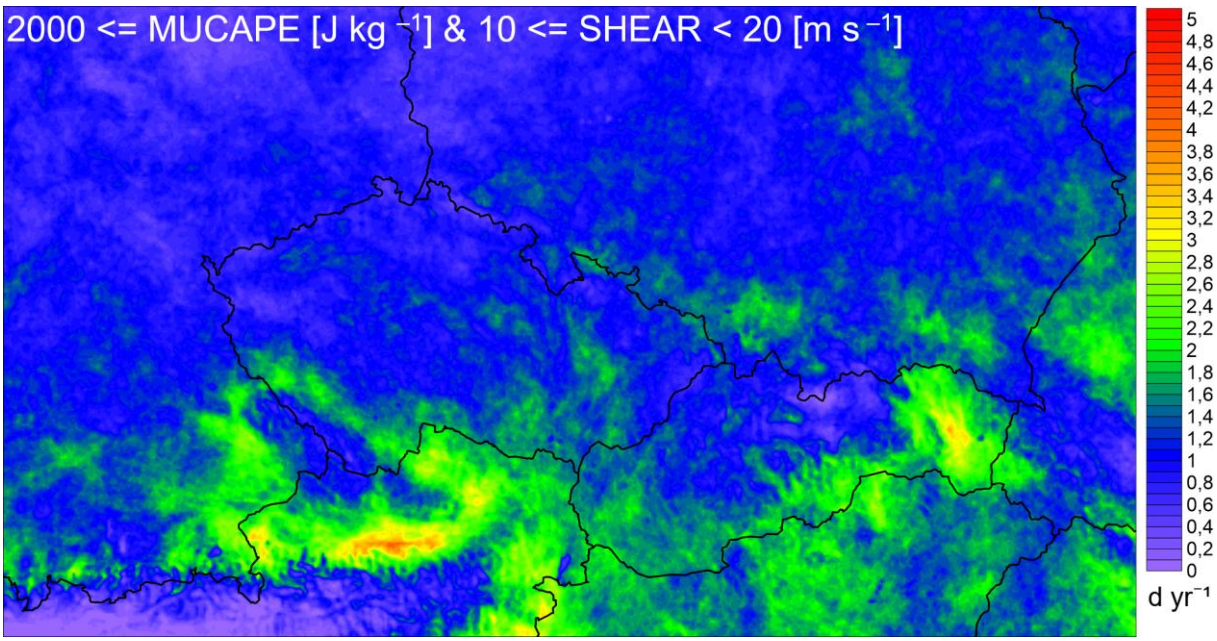


Fig. 5. As in Fig. 3, but for the MUCAPE and 0–6-km bulk wind shear criteria specified in the figure title.

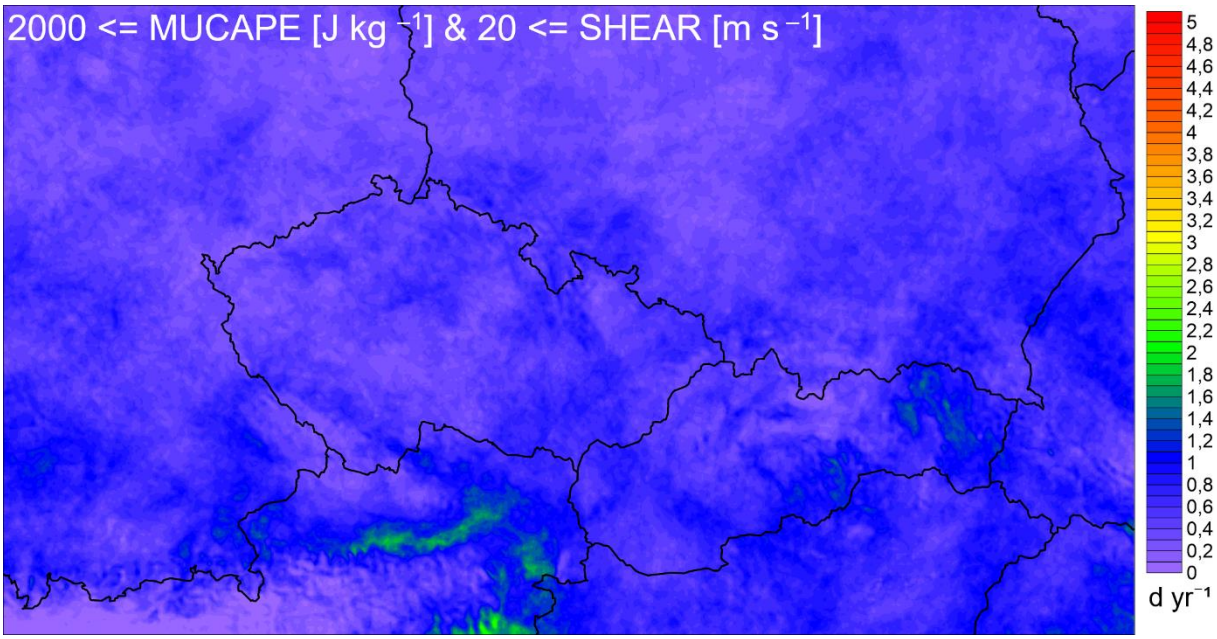


Fig. 6. As in Fig. 3, but for the MUCAPE and 0–6-km bulk wind shear criteria specified in the figure title.

The spatial analysis of convective precursors indicates that very high instability and strong deep-layer shear have limited climatological overlap, as their preferred regions and periods do not necessarily coincide. Within the analyzed combinations, strong-shear environments occur considerably more frequently with moderate MUCAPE, whereas very high MUCAPE is more commonly accompanied by moderate shear. This pattern is consistent with the distinction between high-shear, lower-CAPE and high-CAPE, lower-shear convective regimes described in previous studies (e.g., Sherburn and Parker 2014). However, these categories describe environmental favorability only, as storm mode also depends on the vertical wind-profile shape, forcing, convective inhibition, and storm interactions (Ribeiro and Bosart 2018).

Local maxima in the frequency of the combined environments recur in the northeastern Alpine foreland, near the southern margins of the Czech Republic, along the northern Carpathian foreland, and in southern and eastern Slovakia. These regions broadly correspond to areas previously associated with enhanced convective initiation or severe weather near complex terrain (e.g., Kvak et al. 2023; Fischer et al. 2025). Orographic effects may enhance such environments through thermally driven upslope flows, moisture transport, and the formation of convergence zones. Frequencies are generally lower over the highest Alpine and Carpathian terrain, likely reflecting cooler conditions and reduced moisture availability. The overall patterns suggest interactions among terrain elevation, regional moisture and instability gradients, and terrain-modified wind fields. Orography may also enhance wind shear locally by altering low-level wind direction and speed (Trapp et al. 2020). However, the maps alone neither establish a causal orographic influence nor indicate that convection developed on the identified days.

Conclusions

The ALADIN regional reanalysis provides a detailed representation of convective environments over the Czech Republic, Slovakia, and surrounding regions. Comparison with radiosonde profiles from Praha–Libuš showed that ALADIN reproduced the observed MUCAPE category in approximately two-thirds of cases and identified most strongly unstable environments. However, MUCAPE was more frequently assigned to higher categories than in the observations, indicating a tendency to overestimate the occurrence of strong instability at this station. The spatial climatology revealed pronounced contrasts between mountains, foothills, and lowlands. The highest values within the upper range of daily maximum MUCAPE occurred mainly in lowland and basin regions, whereas the combined occurrence of high instability and strong deep-layer shear showed repeated local maxima near the Alpine and

Carpathian foothills, southern Czechia, and eastern Slovakia. Environments with moderate instability and strong shear were substantially more frequent than those combining high MUCAPE with strong shear, showing that the most favorable thermodynamic and kinematic conditions rarely occur together. Overall, the results highlight the value of kilometre-scale regional reanalysis for resolving fine-scale spatial contrasts in environments supportive of organized and severe convection.

Acknowledgments

The research was partially funded by the Technology Agency of the Czech Republic (grant no. SS02030040, PERUN).

References

Doswell, C. A., Brooks, H. E., Maddox, R. A., 1996. Flash Flood Forecasting: An Ingredients-Based Methodology. *Wea. Forecasting*, **11**, pp. 560–581. https://doi.org/10.1175/1520-0434(1996)011<0560:FFFAIB>2.0.CO;2

Dotzek, N., Groenemeijer, P., Feuerstein, B., Holzer, A. M., 2009. Overview of ESSL's severe convective storms research using the European Severe Weather Database ESWD. *Atmos. Res.*, **93**, pp. 575–586. https://doi.org/10.1016/j.atmosres.2008.10.020

Fischer, J., et al., 2025. Invited perspectives: Thunderstorm Intensification from Mountains to Plains. *Nat. Hazards Earth Syst. Sci.*, **25**, pp. 2629–2656. https://doi.org/10.5194/nhess-25-2629-2025

Groenemeijer, P., et al., 2017. Severe Convective Storms in Europe: Ten Years of Research and Education at the European Severe Storms Laboratory. *Bull. Amer. Meteor. Soc.*, **98**, pp. 2641–2651. https://doi.org/10.1175/BAMS-D-16-0067.1

Kühne, T., Antonescu, B., Groenemeijer, P., Púčik, T., 2025. Lightning Fatalities in Europe (2001–20). *Weather, Climate, and Society*, **17**, pp. 205–215. https://doi.org/10.1175/WCAS-D-24-0038.1

Kvak, R., Okon, Ľ., Bližňák, V., Méri, L., Kašpar, M., 2023. Spatial distribution and precipitation intensity of supercells: Response to terrain asymmetry in the Western Carpathians, Central Europe. *Atmos. Res.*, **292**, 106885. https://doi.org/10.1016/j.atmosres.2023.106885

Kvak, R., Kašpar, M., 2026. Orographically induced flows contributing to convective storm initiation: A review. *AUC GEOGR.*, e23361980.2026.7. https://doi.org/10.14712/23361980.2026.7

Mulholland, J. P., Nesbitt, S. W., Trapp, R. J., Rasmussen, K. L., Salio, P. V., 2018. Convective Storm Life Cycle and Environments near the Sierras de Córdoba, Argentina. *Mon. Wea. Rev.*, **146**, pp. 2541–2557. https://doi.org/10.1175/MWR-D-18-0081.1

Nelson, T. C., Marquis, J., Varble, A., Friedrich, K., 2021. Radiosonde Observations of Environments Supporting Deep Moist Convection Initiation during RELAMPAGO-CACTI. *Mon. Wea. Rev.*, **149**, pp. 289–309. https://doi.org/10.1175/MWR-D-20-0148.1

Púčik, T., Castellano, C., Groenemeijer, P., Kühne, T., Rädler, A. T., et al., 2019. Large Hail Incidence and Its Economic and Societal Impacts across Europe. *Mon. Wea. Rev.*, **147**, pp. 3901–3916. https://doi.org/10.1175/MWR-D-19-0204.1

Ribeiro, B. Z., Bosart, L. F., 2018. Elevated Mixed Layers and Associated Severe Thunderstorm Environments in South and North America. *Mon. Wea. Rev.*, **146**, pp. 3–28. https://doi.org/10.1175/MWR-D-17-0121.1

Sherburn, K. D., Parker, M. D., 2014. Climatology and Ingredients of Significant Severe Convection in High-Shear, Low-CAPE Environments. *Wea. Forecasting*, **29**, pp. 854–877. https://doi.org/10.1175/WAF-D-13-00041.1

Taszarek, M., Brooks, H. E., Czernecki, B., 2017. Sounding-Derived Parameters Associated with Convective Hazards in Europe. *Mon. Wea. Rev.*, **145**, pp. 1511–1528. https://doi.org/10.1175/MWR-D-16-0384.1

Taszarek, M., Brooks, H. E., Czernecki, B., Szuster, P., Fortuniak, K., 2018. Climatological Aspects of Convective Parameters over Europe: A Comparison of ERA-Interim and Sounding Data. *J. Climate*, **31**, pp. 4281–4308. https://doi.org/10.1175/JCLI-D-17-0596.1

Taszarek, M., et al., 2019. A Climatology of Thunderstorms across Europe from a Synthesis of Multiple Data Sources. *J. Climate*, **32**, pp. 1813–1837. https://doi.org/10.1175/JCLI-D-18-0372.1

Taszarek, M., Allen, J. T., Púčik, T., Hoogewind, K. A., Brooks, H. E., 2020. Severe Convective Storms across Europe and the United States. Part II: ERA5 Environments Associated with Lightning, Large Hail, Severe Wind, and Tornadoes. *J. Climate*, **33**, pp. 10263–10286. https://doi.org/10.1175/JCLI-D-20-0346.1

Trapp, R. J., et al., 2020. Multiple-Platform and Multiple-Doppler Radar Observations of a Supercell Thunderstorm in South America during RELAMPAGO. Mon. *Wea. Rev.*, **148**, pp. 3225–3241. https://doi.org/10.1175/MWR-D-20-0125.1